DOI: 10.13009/EUCASS2023-913
Aerospace Europe Conference 2023 – 10TH EUCASS – 9TH CEAS

Closed-loop control of an open-cavity flow with magnetically actuated microvalves

Thomas ARNOULT [*†], *Colin Leclercq* [**], *Charles Poussot-Vassal* [***], *Cécile Ghouila-Houri* [*], *Aurélien Mazzamurro* [*], *Alain Merlen* [*], *Eric Garnier* [****], *Denis Sipp* [**], *Philippe Pernod* [*], *Abdelkrim Talbi* [*]

[*] *Univ. Lille, CNRS, Centrale Lille, Yncréa ISEN, Univ. Polytechnique Hauts-de-France, UMR 8520 IEMN, F-59000 Lille, France,* thomas.arnoult@centralelille.fr, cecile.ghouila@centralelille.fr, aurelien.mazzamurro@centralelille.fr, alain.merlen@univ-lille.fr, philippe.pernod@centralelille.fr, abdelkrim.talbi@univ-lille.fr

[**] *DAAA, ONERA The French Aerospace Lab, Meudon, F-92190, France,* colin.leclercq@onera.fr, *denis.sipp@onera.fr*

[***] *DTIS, ONERA - The French Aerospace Lab, F-31055 Toulouse, France,* Charles.Poussot-Vassal@onera.fr

[****] *Univ. Lille, CNRS, ONERA, Arts et Metiers Institute of Technology, Centrale Lille, UMR 9014, Laboratoire de Mécanique des fluides de Lille—Kampé de Fériet, F-59000 Lille, France,* eric.garnier@onera.fr

† Corresponding Author

Abstract

In this paper, a linear array of 15 MMMS (Micro-Magneto-Mechanical Systems) microvalves is integrated to an open-cavity upstream edge to perform closed-loop flow control experiments. The microvalves can generate both quasi-steady and pulsed jets and have the advantage to be able to follow arbitrary command signals, which is a key for closed-loop flow control. For a freestream velocity of 20 m/s, the open-cavity flow is characterized by a resonant frequency of 128.6 Hz, which sound pressure level is reduced in closed-loop by 9 dB for a total flow rate of 10 L/min.

1. Introduction

The open-cavity is a commonly studied geometry in flow control applications. Its dynamics has been studied since Roshko [1], Pereira [2] or Plumblee et al [3] and makes it a convenient test-bed for new actuators or control approaches. The complex dynamics developing in an open-cavity flow has been described by Rossiter [4] and consists in a boundary layer developing upstream the cavity, separating at the upstream corner and forming the shear layer, as sketched in Figure 1. This shear layer undergoes hydrodynamic instabilities over the cavity and impacts the downstream corner of the cavity, where acoustic waves are generated. They propagate upstream the cavity and excite the shear layer instabilities.

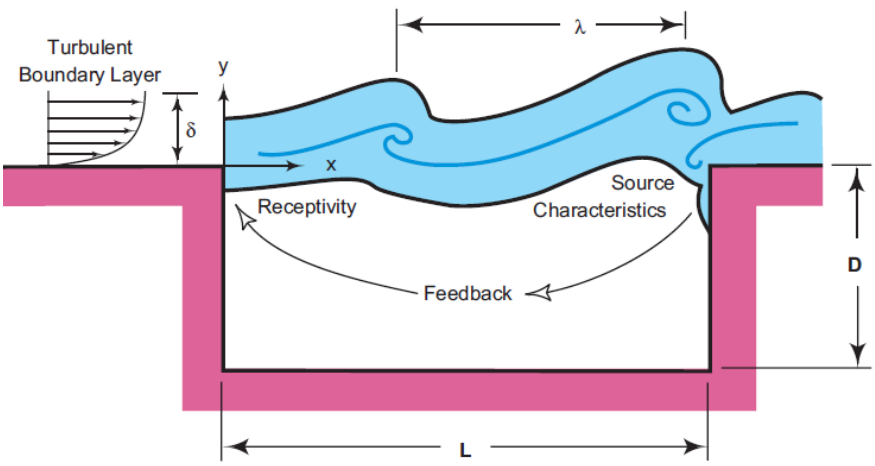

Figure 1: Illustration of the flow developing over an open-cavity [5]

DOI: 10.13009/EUCASS2023-913

The self-sustained oscillations in the open-cavity flow are therefore due to an aero-acoustic feedback mechanism. Rossiter [4] proposed an empirical expression for the prediction of the oscillation frequencies in the case of subsonic and transonic flows, such that:

$$f = \frac{U_\infty}{L}\,\frac{(m-\gamma)}{(\frac{1}{\kappa}+M)} \tag{1}$$

where U_∞, L and M respectively denote the freestream velocity, the cavity length and the flow Mach number. The quantities m, κ and γ respectively stand for the mode number, the ratio between the convection speed of the vortices in the shear layer and the freestream velocity and model of a time delay betwee, the vortex impact and the emission of an acoustic wave. To tune the empirical model in Equation 1, values of κ and γ were set to 0.57 and 0.25. Considering incompressible cases of flow past open-cavities, Rockwell [6] and Rockwell and Naudascher [7,8] adapted the semi-empirical Rossiter mode equation according to:

$$f = \frac{U_\infty}{L}\,(m-\gamma)\kappa \tag{2}$$

For deep open-cavities, the feedback mechanism can be coupled with an acoustic resonance mechanism due to the cavity normal acoustic modes. This particular mechanism was investigated by East [9], who proposed the following equation to predict the fundamental resonance frequency f:

$$f = \frac{a}{D}\,\frac{0.25}{1+A\left(\frac{L}{D}\right)^{B}} \tag{3}$$

with A, B empirical coefficients and a the speed of sound. In this formula, the freestream velocity does not play a role but only the cavity dimensions and the speed of sound indicating a purely acoustic mode. Both Rossiter and East modes can interact with each other, yielding a local maximum in the global modes growth rate of instabilities of the base flow. For low Mach numbers the latter mechanism can be seen as enhancing the former mechanism response, as shown by Yamouni *et al* [10]. Both mechanisms result in the generation of flow-induced noise radiation and structural vibrations, which could damage structures.

Flow control can be defined, as proposed by MacMynowski and Williams [11], as modifying a flow behavior in order to obtain positive changes. In the case of an open-cavity flow, the aim is to damp the flow oscillations. This control relies on the suppression of the flow feedback mechanisms by interactions of actuators with the upstream boundary layer, as performed by Vakili and Gauthier [12], or by interactions of induced flow perturbations with the shear layer at the upstream edge of the open-cavity, as implemented by Ukeiley *et al* [13], Shaw [14], Stanek *et al* [15], Sarno and Franke [16] or Cattafesta *et al* [17]. Different closed-loop control approaches have been employed targeting the suppression of open-cavity flow oscillations. The first experiments consisted in tuning open-loop forcing parameters in a quasi-static fashion, based on the information fed back from a performance sensor, as carried out by Gharib [18], Shaw and Northcraft [19], Micheau *et al* [20] or Debiasi and Samimy [21]. With promising results, as described in the following, control of open-cavity flows then moved to closed-loop control from estimation sensors, requiring less power to control the flow than quasi-static approaches. Closed-loop methods can rely on black bock models of the input-output dynamics using adaptive filters approaches [22] or using the frequency response of the sensors to an excitation of the actuators [23] or be model-free as this is the case concerning machine-learning approaches [24].

In this paper, we integrate a linear array of 15 MMMS (Micro-Magneto-Mechanical Systems) microvalves [25] to an open-cavity upstream edge to perform closed-loop flow control experiments. The microvalves can generate both quasi-steady and pulsed jets and have the advantage to be able to follow arbitrary command signals, which is a key for closed-loop flow control. This paper second part describes the MMMS microvalves technology, while the third part deals with the open-cavity flow characterization and closed-loop control implementation.

2. Microvalves architecture and characterization

2.1 Microvalves architecture

The considered microvalve architecture is presented in Figure 2 and consists of two parts, based on the micromachining of silicon layers and of PDMS (Polydimethylsiloxane) seals, ensuring the microvalve airtightness. The assembling of the two parts define the air inlet, the microchannel with inner walls and the air outlet. The microchannel is surmounted

DOI: 10.13009/EUCASS2023-913

by a rigid silicon pad, with permanent magnets fixed over it. The microvalve packaging contains a coil surrounding the magnets. This actuator design enables to generate two different type of jets: quasi-steady jets and pulsed jets. To generate quasi-steady jets, a pressure difference $\Delta P = P_{in} - P_{atm}$ is applied through the microvalve. The rigid silicon pad is then lifted up to an equilibrium position and air flows from the inlet to the outlet.

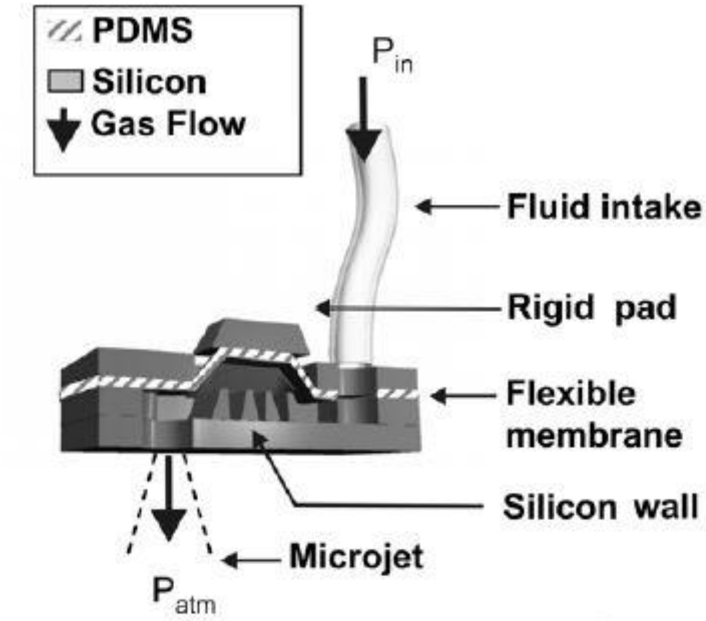

Figure 2: General design of the microvalves architecture [26]

To generate pulsed jet, a pressure difference is still applied through the microvalve. In addition, a current runs in the coil surrounding the magnets, inducing a magnetic field moving the rigid silicon pad up and down, as depicted in Figure 3. Consequently, the microchannel height is modulated resulting in the generation of a pulsed jet at the actuator outlet.

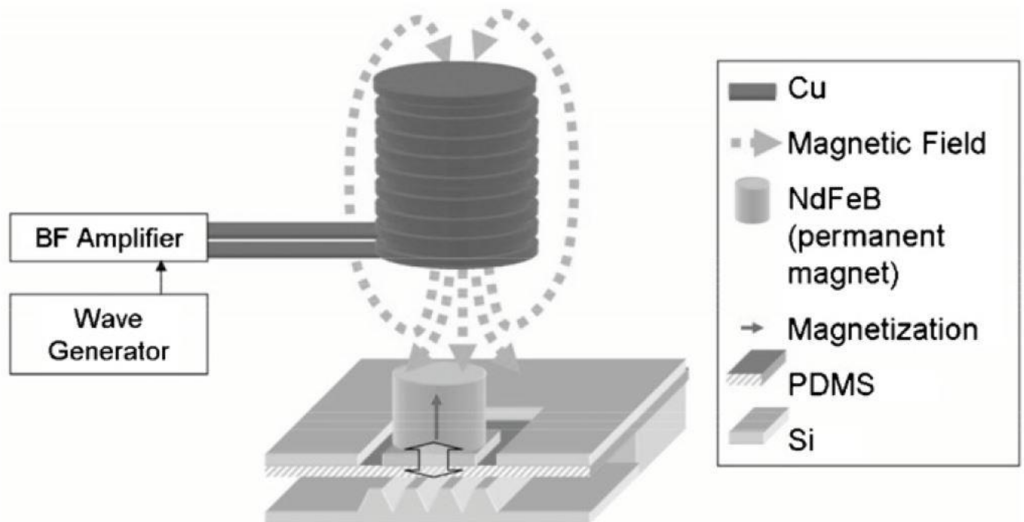

Figure 3: Sketch of the microvalve with a current running in the coil to generate pulsed jets [26]

In order to adapt the microvalve outlet to the open-cavity geometry, the outlet hole was transformed into a slot outlet. The adapter is fabricated by stereolithography in a Problack10 resin. It is composed of an upper and a lower part, which brought together induce a jet outlet angle of 45°, as pictured in Figure 4.

DOI: 10.13009/EUCASS2023-913

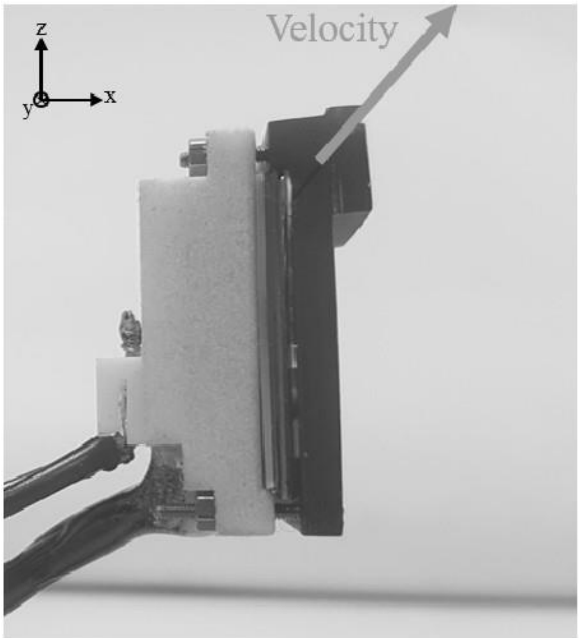

Figure 4: Assembled microvalve with is packaging and the jet adapter

2.2 Quasi-steady and pulsed jets characterization

In order to perform the closed-loop flow control experiments, a set of 15 microvalves is assembled and integrated as a linear array. Hot-wire measurements are performed to characterize both quasi-steady and pulsed jets. A Dantec 55P11 hot wire probe associated to a mini CTA 54T42 is used to perform measurements with a sampling frequency of 20 kHz over 1 s at each considered point. Measurements are carried out in the (XZ) planes, sketched in Figure 4, where X, Y and Z axes are defined with respect to the actuators outlet. The flow crosses the (XZ) measurement plane with a 45° angle. The hot wire probe is placed parallel to the Y axis. Hence, the velocity measured by the hot wire is a combination of the X and Z velocity components. One microvalve is supplied with a pressure difference of $\Delta P = 150$ mbar. These measurements are presented in Figure 5. Based on these measurements, the outlet jet angle induced by the adapter could be measured and revealed to be 45° as expected based on the adapter design.

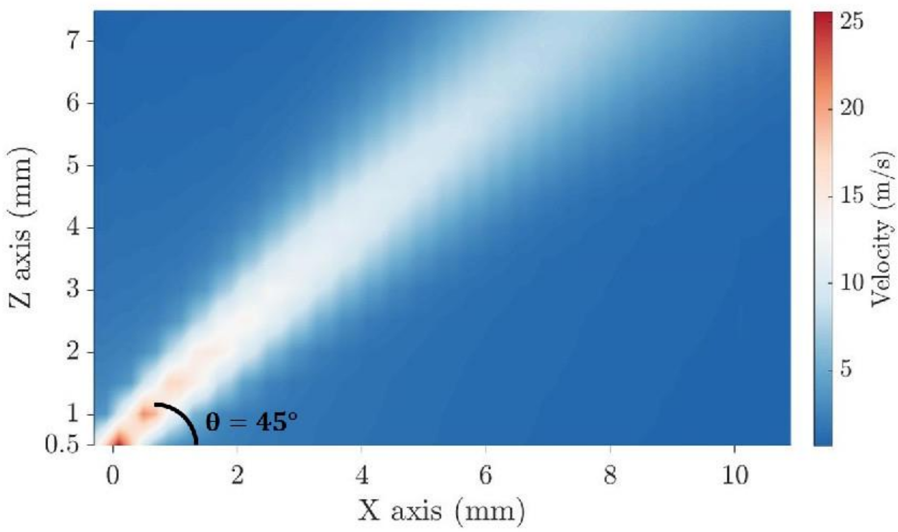

Figure 5: Quasi-steady jet mapping in the (XZ) plane for $\Delta P = 150$ mbar

Pulsed jets are also characterized with hot wire measurements, the sensor being placed at the microvalve maximum velocity location for X=0.5 mm. The entire array of actuators is fed with a pressure difference $\Delta P = 250$ mbar. Figure 6 illustrates such a measurement for a forcing frequency of 40 Hz. The pulsed jet consists indeed in a modulation of the outlet velocity around a mean value. Microvalves pulsed jets were characterized for actuation frequencies between

DOI: 10.13009/EUCASS2023-913

20 Hz and 380 Hz. All the tested actuators proved to behave linearly on the tested bandwidth. Furthermore, the microvalves proved to have the advantage to be able to follow arbitrary command signals, which is a key for closed-loop flow control.

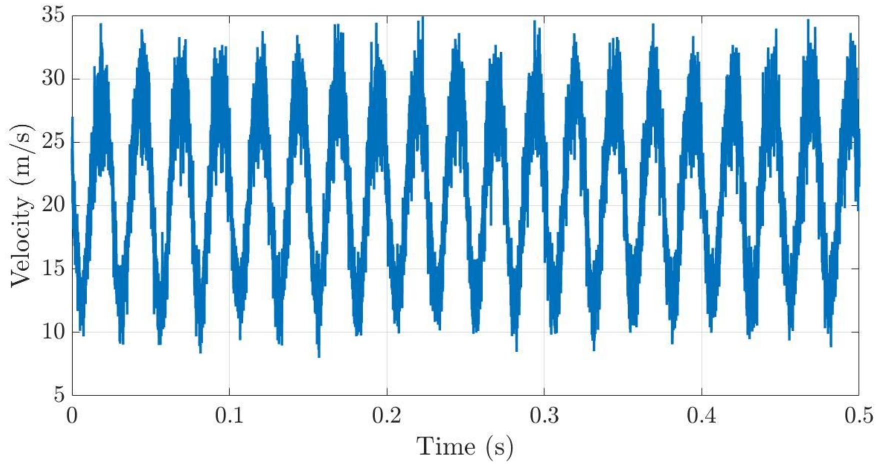

Figure 6: Hot wire velocity measurement for an input signal frequency of 40 Hz

3. Closed-loop control of the open-cavity flow

3.1 Wind tunnel facility

The wind tunnel test section has a rectangular shape of height 150 mm and span 300 mm, for a total length of 1910 mm. The cavity geometry is characterized by a length of 134 mm and a depth of 900 mm. The linear array of 15 microvalves was integrated to the open-cavity placed in the ONERA S19 wind tunnel. A picture of the wind tunnel and of the actuators integration is presented in Figure 7. Kulite XCQ-093-15A (15 PSI) pressure sensors are integrated to the open-cavity downstream wall in order to perform unsteady pressure measurements. These measurements help characterizing the unforced flow dynamics and are used to implement the closed-loop control. Data acquisition and signal generation are performed with a Dspace MicroLabBox real time controller composed of a 2 GHz dual core DS1202 processor with a 16 bits on ± 10 V range analog-to-digital converter.

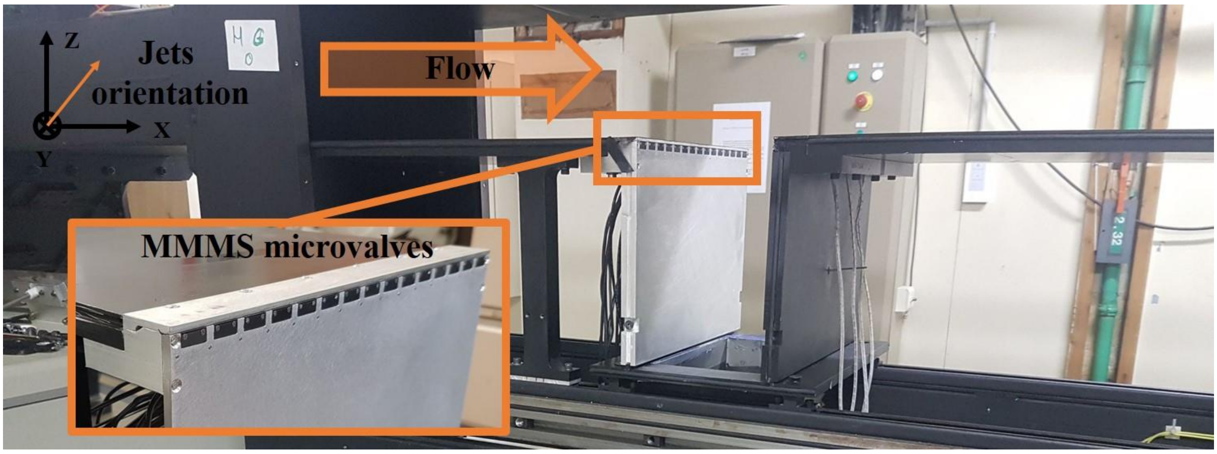

Figure 7: Integration the array of MMMS microvalves to the open-cavity

3.2 Open-cavity unforced flow characterization

Characterization of the flow dynamics is investigated for several freestream velocities U_∞ with the aim of finding a flow regime with low frequency oscillations inside the actuators bandwidth. The SPL (Sound Pressure Level),

DOI: 10.13009/EUCASS2023-913

expressed in dB, obtained from the PSD (Power Spectral Density) of each Kulite sensors are computed based on the following definition:

$$\mathrm{SPL} = 20log_{10}\left(\frac{\sqrt{PSD}}{P_{ref}}\right), \quad (4)$$

where $P_{ref} = 20$ µPa is a reference pressure corresponding to the threshold of human hearing. In the following, unless otherwise specified, unsteady pressure signals are acquired over a duration of 45 s with a sampling frequency $f_s = 10$ kHz. The signal PSD is then computed with a Welch's algorithm based on 60 Hamming windows and an overlap of 50%, yielding a frequency resolution of 0.11 Hz. As the 4 Kulite sensors indicate the same resonance frequencies and similar values of SPL within a few dB, results presented in the following are based on one of the 4 unsteady pressure sensors. The open-cavity spectrum derived for a freestream velocity $U_\infty = 20$ m/s is presented in Figure 8. It is composed of a parasitic peak at 50 Hz due to electrical noise and one peak entirely characterizing the flow dynamics. The flow spectrum is therefore composed of a fundamental oscillation frequency at 128.6 Hz. This flow regime is the one considered to carry out the closed-loop control experiments.

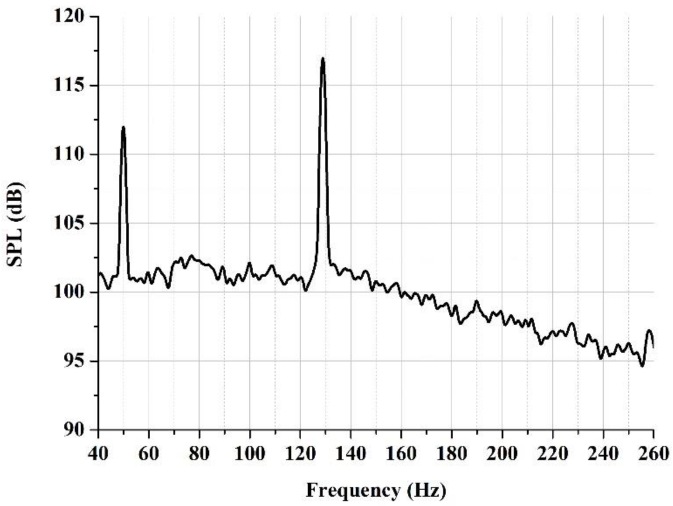

Figure 8: Evolution of the SPL (dB) against the frequency for a freestream velocity $U_\infty = 20$ m/s

3.3 Closed-loop control of the open-cavity flow

The SISO (Single Input Single Output) closed-loop control of the open-cavity flow is based on the mixed sensitivity formulation of a H_∞ loop-shaping approach. The closed-loop control strategy therefore boils down to three steps: first identifying a transfer function between the actuators command and the selected Kulite sensor output, second deriving an optimized controller based on the H_∞ loop-shaping approach and third implementing the controller into the Dspace real-time unit. The following results of the closed-loop control implementation are described for a driving pressure of the actuators of 120 mbar.

3.3.1 Identification of a transfer function

The identification of a transfer function between the actuators and the sensor output is performed using linear frequency sweeps, described by the following equations:

$$f_{act} = Asin(2\pi\left(f_{start} + \frac{f_{stop}-f_{start}}{\Delta t}t\right)t), \quad (5)$$

where f_{act}, $A = 2$ V, $f_{start} = 120$ Hz, $f_{stop} = 260$ Hz, Δt and t respectively denote the instantaneous actuation frequency, the signal amplitude, the linear sweep starting and stopping frequencies, the linear sweep duration and the instantaneous time. Using 3 realizations of such a sweep, an average response of the open-cavity to the forcings is computed. Figure 9 highlights the gathered frequential data gain and phase.

DOI: 10.13009/EUCASS2023-913

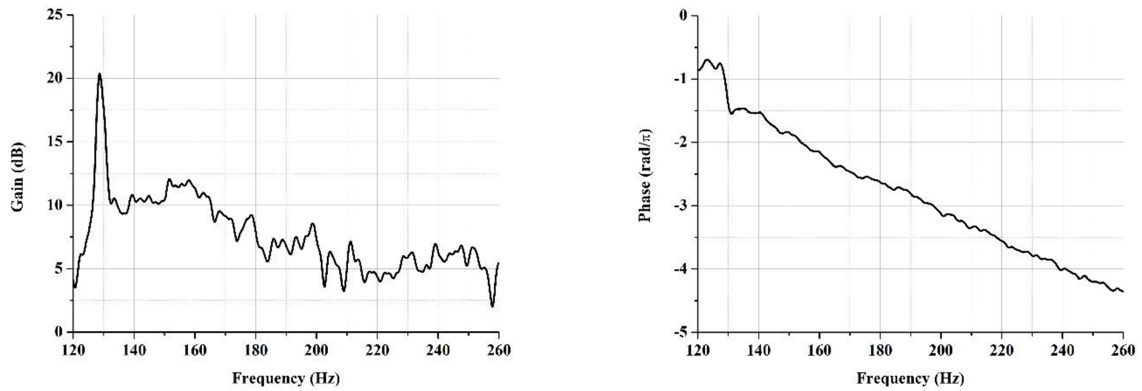

Figure 9: Gain (left) and phase (right) of the average frequency response of the open-cavity flow for $U_\infty = 20$ m/s and $\Delta P = 120$ mbar

As expected in the gain plot, a resonance appears at the open-cavity resonant frequency of 128.6 Hz. Furthermore, considering the phase plot, a change in the phase is observed around the resonant frequency. The phase linear decrease is related to a delay τ associated to the advection of the flow perturbations along the cavity in the shear layer with a mean velocity κU_∞. Based on the measurements presented in Figure 9, $\kappa = 0.57$ indicating that the pertubations induced by the actuators are convected inside the flow with a mean velocity of $0.57U_\infty$. This value is in close agreement with values found in the literature [23,27].

Based on these frequential data, an interpolated transfer function is built using the Matlab “n4sid” routine in order to derive a discrete-time state-space model of order 10. In Figure 10, the state-space model gain follows the gain trend of the average frequency response, while the phase is matched with even greater precision. The transfer function fit is estimated at 80.9 %, according to the normalized RMS (root mean square) error. This interpolated transfer function is then used for the synthesis of the controller.

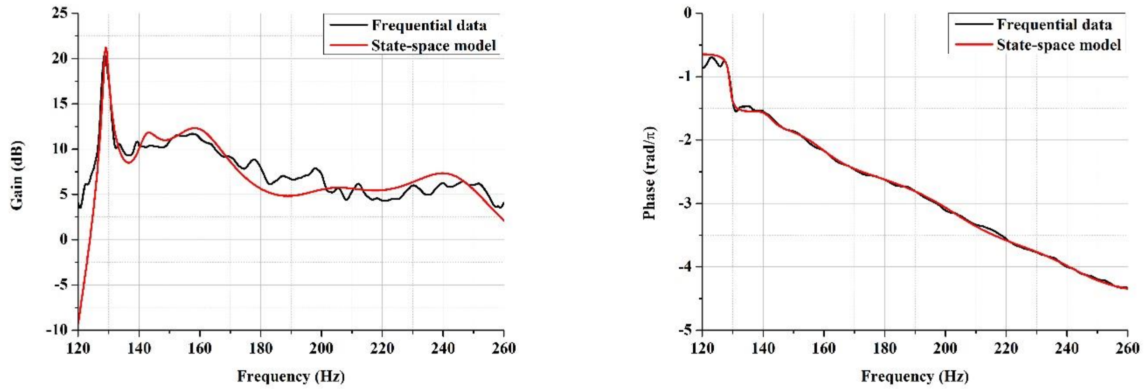

Figure 10: Gain (left) and phase (right) of the average frequency response (black) and interpolated transfer function (red) of the open-cavity flow for $U_\infty = 20$ m/s and $\Delta P = 120$ mbar

3.3.2 Controller synthesis

Based on the interpolated transfer function, the aim is to design a controller, which closed-loop performance is defined by the user. The design process is based on the mixed-sensitivity formulation of a H_∞ loop-shaping approach. Let S, G and K respectively be the problem sensitivity transfer function, the system closed-loop transfer function and the controller transfer function. A set of weighting transfer functions W_S, W_G and W_K are therefore defined and constitute the basis of the control optimization process. The H_∞ loop-shaping control design approach amounts to minimizing the cost function γ bounding the H_∞ norm of the previous mentioned transfer functions based on the chosen weighting functions. Solved through the “hinfstruct” routine in Matlab, the controller K is sought such that Equation (6) is satisfied and such that the internal dynamics of the system is stabilized.

DOI: 10.13009/EUCASS2023-913

$$\begin{cases} \|W_S S\|_\infty < \gamma \\ \|W_G G\|_\infty < \gamma. \\ \|W_K K\|_\infty < \gamma \end{cases} \quad \textbf{(6)}$$

Running the "hinfstruct" routine, on the previously presented study case, yields $\gamma = 0.71$. The optimized is then implemented into a Simulink code and transferred onto the Dspace MicroLabBox real time controller. The considered Kulite sensor for the SISO approach is used as the system input and the command signal issued by the controller is used to drive the array of microvalves.

3.3.3 Closed-loop control application

Figure 11 compares the cavity spectra for $U_\infty = 20$ m/s and $\Delta P = 120$ mbar in the closed-loop case. The cavity dynamics without forcing corresponds to the black curve, which exhibits the open-cavity resonance at $f = 128.6$ Hz for a SPL of 117 dB. The blue curve corresponds to the open-loop forcing of the cavity with the quasi-steady jets for $\Delta P = 120$ mbar. In this case, the cavity resonance is only damped by 1 dB. This low damping of the resonance in open-loop is chosen in order to highlight the effect of the closed-loop control. The red curve describes the closed-loop case for which the cavity resonance is damped by 9 dB compared to the open-loop case. The closed-loop control strongly dampens the cavity resonance.

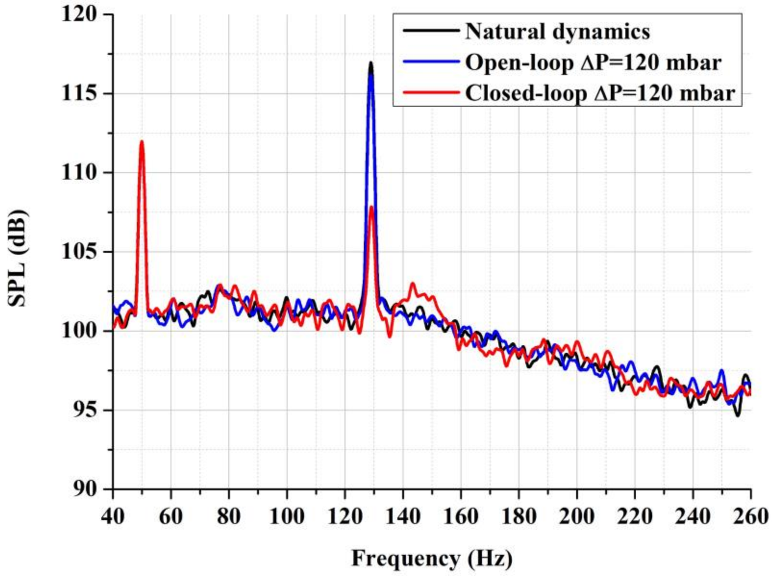

Figure 11: SPL (dB) flow spectrum of the open-cavity for $U_\infty = 20$ m/s and $\Delta P = 120$ mbar in the unforced case (black), open-loop case (blue) and closed-loop case (red)

The electrical power consumption derived from the microvalves command and intensity records indicates a mean consumption of 1.5 W for the array of 15 microvalves, yielding an average consumption of 0.1 W per actuator. This study case shows the straightforward use of the MMMS microvalves in the closed-loop control of a periodic open-cavity flow.

4. Conclusion

In this paper, MMMS microvalves employed in closed-loop flow control experiments on an open-cavity are presented. Their design enables to generate both quasi-steady and pulsed jets, consisting of a modulation of the outlet velocity around a mean value. Characterized with hot wire measurements, microvalves proved to behave linearly on a large bandwidth. Because of this linear behaviour, the MMMS microavles have the advantage to be able to follow arbitrary command signals, which is a key for the implementation of closed-loop flow control experiments. Integrated as a linear array to the open-cavity upstream edge and used during closed-loop control the experiments, the MMMS microvalves

DOI: 10.13009/EUCASS2023-913

damped the open-cavity resonance SPL by 9 dB. This study constitutes a first step towards the closed-loop control of more complex flows such as quasi-periodic open-cavity flows.

References

[1] A. Roshko, 'Some measurements in a rectangular cutout', National Advisory committee for aeronautics, Technical note 3488, 1955.

[2] J. C. F. Pereira and J. M. M. Sousa, 'Experimental and Numerical Investigation of Flow Oscillations in a Rectangular Cavity', Journal of Fluids Engineering, vol. 117, no. 1, pp. 68–74, Mar. 1995

[3] Plumblee, Gibson, and Lassiter, 'A theoretical and experimental investigation of the acoustic response of cavities in an aerodynamic flow', Marietta, Georgie, Technical report WADD-61-75.

[4] J. E. Rossiter, 'Wind tunnel experiments on the flow over rectangular cavities at subsonic and transonic speeds', RAE Technical Report No. 64037, 1964.

[5] L. N. Cattafesta, Q. Song, D. R. Williams, C. W. Rowley, and F. S. Alvi, 'Active control of flow-induced cavity oscillations', Progress in Aerospace Sciences, vol. 44, no. 7–8, pp. 479–502, Oct. 2008.

[6] D. Rockwell. Prediction of Oscillation Frequencies for Unstable Flow Past Cavities. Journal of Fluids Engineering, 99(2):294–299, June 1977.

[7] D Rockwell and E Naudascher. Self-Sustained Oscillations of Impinging Free Shear Layers. Annual Review of Fluid Mechanics, 11(1):67–94, January 1979.

[8] D. Rockwell and E. Naudascher. Review—Self-Sustaining Oscillations of Flow Past Cavities. Journal of Fluids Engineering, 100(2):152–165, June 1978.

[9] L.F. East. Aerodynamically induced resonance in rectangular cavities. Journal of Sound and Vibration, 3(3):277–287, May 1966.

[10] Sami Yamouni, Denis Sipp, and Laurent Jacquin. Interaction between feedback aeroacoustic and acoustic resonance mechanisms in a cavity flow: a global stability analysis. Journal of Fluid Mechanics, 717:134–165, February 2013.

[11] G MacMynowski, D and D Williams. Flow Control Terminology, Fundamentals and Applications of Modern Flow Control. AIAA Journal, pages 59–71, 2009.

[12] Ahmad D. Vakili and Christian Gauthier. Control of cavity flow by upstream massinjection. Journal of Aircraft, 31(1):169–174, January 1994.

[13] Lawrence Ukeiley, Michael Sheehan, Francois Coiffet, Farrukh Alvi, Srinivasan Arunajatesan, and Bernard Jansen. Control of Pressure Loads in Geometrically Complex Cavities. Journal of Aircraft, 45(3):1014–1024, May 2008.

[14] Leonard Shaw. Active control for cavity acoustics. In 4th AIAA/CEAS Aeroacoustics Conference, Toulouse,France, June 1998. American Institute of Aeronautics and Astronautics.

[15] Michael Stanek, Ganesh Raman, Valdis Kibens, John Ross, Jessaji Odedra, and James Peto. Control of cavity resonance through very high frequency forcing. In 6th Aeroacoustics Conference and Exhibit. American Institute of Aeronautics and Astronautics, 2000.

[16] R. L. Sarno and M. E. Franke. Suppression of flow-induced pressure oscillations in cavities. Journal of Aircraft, 31(1):90–96, January 1994.

[17] L. Cattafesta, III, S. Garg, M. Choudhari, F. Li, L. Cattafesta, III, S. Garg, M. Choudhari, and F. Li. Active control of flow-induced cavity resonance. In 28th Fluid Dynamics Conference, Snowmass Village,CO,U.S.A., June 1997. American Institute of Aeronautics and Astronautics.

[18] M Gharib. Response of the Cavity Shear Layer Oscillations to External Forcing. In AIAA journal, volume 25. American Institute of Aeronautics and Astronautics, 1987.

[19] Leonard Shaw and Stephen Northcraft. Closed loop active control for cavity acoustics. In 5th AIAA/CEAS Aeroacoustics Conference and Exhibit, Bellevue,WA,U.S.A., May 1999. American Institute of Aeronautics and Astronautics.

[20] Philippe Micheau, Ludovic Chatellier, Janick Laumonier, and Yves Gervais. Active Control of a Self-sustained Pressure Fluctuation due to Flow over a Cavity. In 10th AIAA/CEAS Aeroacoustics Conference, Manchester, GREAT BRITAIN, May 2004. American Institute of Aeronautics and Astronautics.

[21] M. Debiasi and M. Samimy. Logic-Based Active Control of Subsonic Cavity Flow Resonance. AIAA Journal, 42(9):1901–1909, September 2004.

[22] Tim Kestens and Franck Nicoud. Active control of an unsteady flow over a rectangular cavity. In 4th AIAA/CEAS Aeroacoustics Conference, Toulouse,France, June 1998. American Institute of Aeronautics and Astronautics.

[23] Colin Leclercq, Fabrice Demourant, Charles Poussot-Vassal, and Denis Sipp. Linear iterative method for closed-loop control of quasiperiodic flows. Journal of Fluid Mechanics, 868:26–65, June 2019.

DOI: 10.13009/EUCASS2023-913

[24] M Efe, Marco Debiasi, Peng Yan, Hitay Ozbay, and Mo Samimy. Control of Subsonic Cavity Flows by Neural Networks - Analytical Models and Experimental Validation. In 43rd AIAA Aerospace Sciences Meeting and Exhibit, Reno, Nevada, January 2005. American Institute of Aeronautics and Astronautics.
[25] P. Pernod et al., ‘MEMS magneto-mechanical microvalves (MMMS) for aerodynamic active flow control’, Journal of Magnetism and Magnetic Materials, vol. 322, no. 9–12, pp. 1642–1646, May 2010.
[26] O Ducloux, R Viard, A Talbi, L Gimeno, Y Deblock, P Pernod, V Preobrazhensky, and A Merlen. A magnetically actuated, high momentum rate MEMS pulsed microjet for active flow control. Journal of Micromechanics and Microengineering, 19(11):115031, November 2009.
[27] Alexandre Barbagallo, Denis Sipp, and Peter J. Schmid. Closed-loop control of an open cavity flow using reduced-order models. Journal of Fluid Mechanics, 641:1–50,December 2009.

Acknowledgments

This work was funded by the French National Research Agency (ANR) in the framework of the ANR ASTRID MATURATION “CAMELOTT-MATVAL” Project. It is supported by the regional platform CONTRAERO, the CPER ELSAT 2020 Project and the CPER RITMEA 2021-2027 Project. The Innovation Defence Agency (AID) has also financially sustained this work. The authors also thank RENATECH, the French national nanofabrication network, and FEDER.